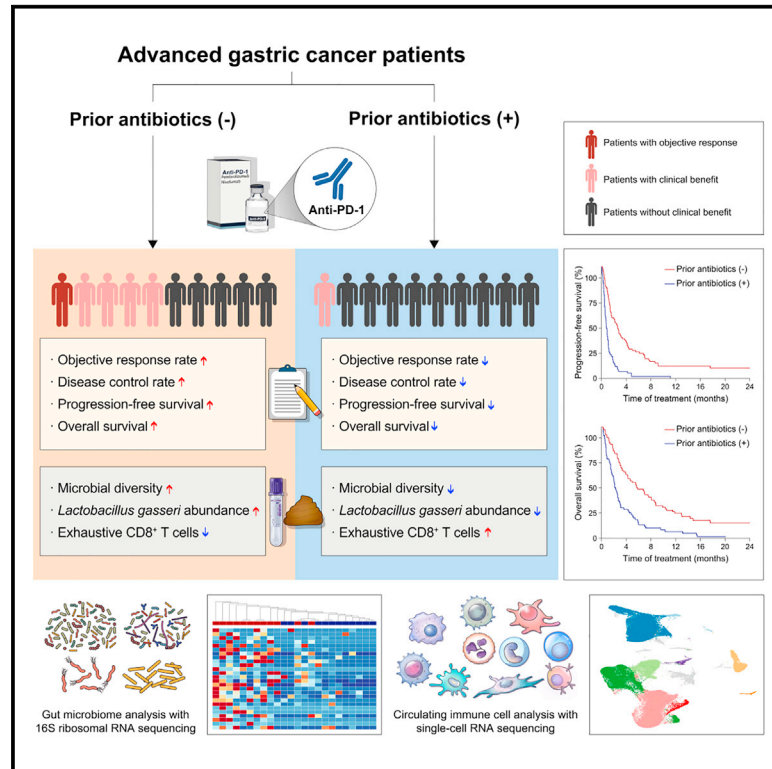


# Prior antibiotic administration disrupts anti-PD-1 responses in advanced gastric cancer by altering the gut microbiome and systemic immune response

## Graphical abstract



## Authors

Chang Gon Kim, June-Young Koh, Su-Jin Shin, ..., Jeong Seok Lee, Young-Do Nam, Minkyu Jung

## Correspondence

jeunghc1123@yuhs.ac (H.-C.J.), chemami@kaist.ac.kr (J.S.L.), youngdo98@krfi.re.kr (Y.-D.N.), minkjung@yuhs.ac (M.J.)

## In brief

Kim et al. demonstrate that prior antibiotic administration is associated with worse outcomes in patients with advanced gastric cancer following PD-1 blockade, which is not recapitulated in patients treated with chemotherapy. Translational analyses reveal that prior antibiotic administration induces dysbiosis of gut microbiota and alteration of systemic immune responses.

## Highlights

- pATBs are associated with inferior outcome in patients with AGC treated with PD-1 blockade
- Outcome of patients with AGC administered chemotherapy is not associated with pATBs
- pATBs diminishes gut microbiome diversity and reduces abundance of *Lactobacillus gasseri*
- pATBs are associated with disproportional enrichment of circulating exhaustive CD8<sup>+</sup> T cells

## Article

# Prior antibiotic administration disrupts anti-PD-1 responses in advanced gastric cancer by altering the gut microbiome and systemic immune response

Chang Gon Kim,<sup>1,13</sup> June-Young Koh,<sup>2,3,13</sup> Su-Jin Shin,<sup>4,13</sup> Ji-Hee Shin,<sup>5,13</sup> Moonki Hong,<sup>1</sup> Hyun Cheol Chung,<sup>1,6</sup> Sun Young Rha,<sup>1,6</sup> Hyo Song Kim,<sup>1</sup> Choong-Kun Lee,<sup>1</sup> Ji Hyun Lee,<sup>1,11</sup> Yejeong Han,<sup>1,12</sup> Hyoyong Kim,<sup>1</sup> Xiumei Che,<sup>1</sup> Un-Jung Yun,<sup>1</sup> Hyunki Kim,<sup>7</sup> Jee Hung Kim,<sup>8</sup> Seo Young Lee,<sup>8</sup> Su Kyoung Park,<sup>9</sup> Sejung Park,<sup>6</sup> Hyunwook Kim,<sup>1</sup> Jin Young Ahn,<sup>10</sup> Hei-Cheul Jeung,<sup>8,\*</sup> Jeong Seok Lee,<sup>2,3,\*</sup> Young-Do Nam,<sup>5,\*</sup> and Minkyu Jung<sup>1,6,14,\*</sup>

<sup>1</sup>Division of Medical Oncology, Department of Internal Medicine, Yonsei Cancer Center, Yonsei University College of Medicine, Seoul, Republic of Korea

<sup>2</sup>Graduate School of Medical Science and Engineering, Korea Advanced Institute of Science and Technology, Daejeon, Republic of Korea

<sup>3</sup>Genome Insight, Inc., Daejeon, Republic of Korea

<sup>4</sup>Department of Pathology, Gangnam Severance Hospital, Yonsei University College of Medicine, Seoul, Republic of Korea

<sup>5</sup>Research Group of Personalized Diet, Korea Food Research Institute, Wanju, Republic of Korea

<sup>6</sup>Songdang Institute for Cancer Research, Yonsei University College of Medicine, Seoul, Republic of Korea

<sup>7</sup>Department of Pathology, Severance Hospital, Yonsei University College of Medicine, Seoul, Republic of Korea

<sup>8</sup>Division of Medical Oncology, Department of Internal Medicine, Gangnam Severance Hospital, Yonsei University College of Medicine, Seoul, Republic of Korea

<sup>9</sup>Department of Medical Records, Severance Hospital, Yonsei University College of Medicine, Seoul, Republic of Korea

<sup>10</sup>Division of Infectious Diseases, Department of Internal Medicine, Severance Hospital, Yonsei University College of Medicine, Seoul, Republic of Korea

<sup>11</sup>Present address: Division of Medical Oncology, Department of Internal Medicine, Eunpyeong St. Mary's Hospital, College of Medicine, The Catholic University of Korea, Seoul, Republic of Korea

<sup>12</sup>Present address: Department of Hematology-Oncology, Inha University College of Medicine, Incheon, Republic of Korea

<sup>13</sup>These authors contributed equally

<sup>14</sup>Lead contact

\*Correspondence: [jeunghc1123@yuhs.ac](mailto:jeunghc1123@yuhs.ac) (H.-C.J.), [chemami@kaist.ac.kr](mailto:chemami@kaist.ac.kr) (J.S.L.), [youngdo98@krfi.re.kr](mailto:youngdo98@krfi.re.kr) (Y.-D.N.), [minkjung@yuhs.ac](mailto:minkjung@yuhs.ac) (M.J.)  
<https://doi.org/10.1016/j.xcrm.2023.101251>

## SUMMARY

Evidence on whether prior antibiotic (pATB) administration modulates outcomes of programmed cell death protein-1 (PD-1) inhibitors in advanced gastric cancer (AGC) is scarce. In this study, we find that pATB administration is consistently associated with poor progression-free survival (PFS) and overall survival (OS) in multiple cohorts consisting of patients with AGC treated with PD-1 inhibitors. In contrast, pATB does not affect outcomes among patients treated with irinotecan. Multivariable analysis of the overall patients treated with PD-1 inhibitors confirms that pATB administration independently predicts worse PFS and OS. Administration of pATBs is associated with diminished gut microbiome diversity, reduced abundance of *Lactobacillus gasseri*, and disproportional enrichment of circulating exhaustive CD8<sup>+</sup> T cells, all of which are associated with worse outcomes. Considering the inferior treatment response and poor survival outcomes by pATB administration followed by PD-1 blockade, ATBs should be prescribed with caution in patients with AGC who are planning to receive PD-1 inhibitors.

## INTRODUCTION

Immune checkpoint inhibitors (ICIs) represent an emerging therapeutic strategy for a broadening range of cancers.<sup>1,2</sup> Administration of ICIs unleashes T lymphocyte-mediated immune responses by inhibiting the interaction between immune checkpoint co-inhibitory receptors and their cognate ligands.<sup>3</sup> Blockade of programmed cell death protein-1 (PD-1) and its ligand programmed death-ligand 1 (PD-L1) is the most widely utilized strategy for reinvigorating exhausted T cells.<sup>4</sup> Several studies have demonstrated the meaningful clinical activity of

the PD-1 inhibitors pembrolizumab and nivolumab among patients with advanced gastric cancer (AGC)<sup>5,6</sup>—the fifth most common cancer and the third most common cause of cancer death globally.<sup>7,8</sup> However, clinical benefits from these agents are largely restricted to a minor proportion of patients,<sup>9,10</sup> necessitating further studies of biomarkers for predicting treatment response, effective combination strategies, and other medical strategies for enhancing therapeutic response.

Primary resistance to ICIs has been associated with low mutation burden,<sup>11</sup> local immunosuppression,<sup>12</sup> exhaustion of tumor-infiltrating lymphocytes,<sup>13</sup> and defective antigen presentation.<sup>14</sup>

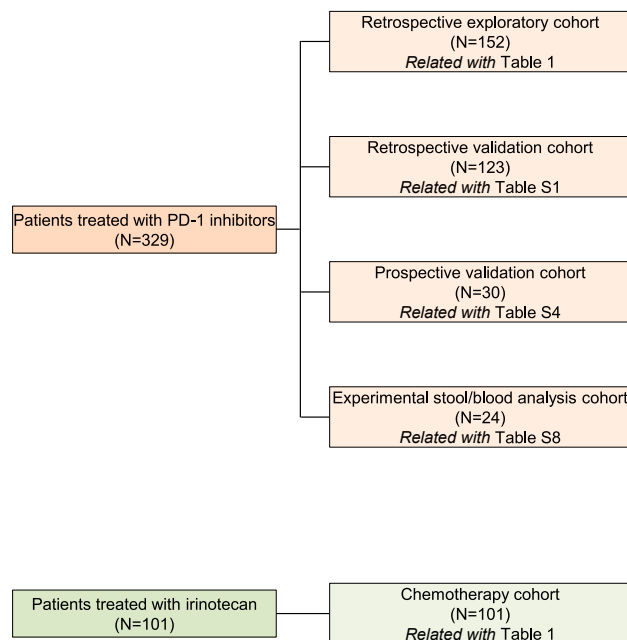


**Figure 1. Schematic description of each cohort**

Recent studies have highlighted the key role of the gut microbiota in shaping antitumor immune responses mediated by ICIs.<sup>15–17</sup> Mechanistically, exposure to broad-spectrum antibiotic (ATB) therapy may adversely influence the therapeutic response to ICIs via modulation of intestinal microbiota.<sup>17–19</sup> Alteration of gut microbiota also influences systemic immune responses, determining anti-PD-1 responses.<sup>20</sup> In accordance with this hypothesis, previous studies have reported that ATB treatment negatively affects the clinical activity of ICIs in patients with non-small cell lung cancer,<sup>21,22</sup> renal cell cancer,<sup>21</sup> and melanoma.<sup>22</sup> In patients with AGC, ATBs are occasionally prescribed during the treatment course.<sup>23</sup> However, no studies to date have vigorously investigated the association between ATB treatment and ICI outcomes in AGC. Furthermore, no studies have addressed whether ATB use is associated with response to PD-1 blockade in a specific manner by comparing outcomes between patients treated with PD-1 inhibitors and those treated with other drugs including chemotherapy.

Therefore, in the present study, we aimed to investigate and validate whether prior ATB (pATB) administration can impair therapeutic response to ICI treatment. In addition, to investigate the clinical implications of ATB treatment according to different treatment strategies, we explored whether the same phenomenon can be observed in patients treated with single-agent chemotherapy with irinotecan. Furthermore, we analyzed circulating immune cells and gut microbiota via single-cell RNA sequencing (scRNA-seq) and 16S ribosomal RNA-seq to provide mechanistic insights correlating pATB administration and outcomes of ICI treatment. Using these approaches with multiple patient cohorts (Figure 1), we thoroughly uncovered clinical and translational evidence that pATB use can influence treatment outcomes of ICI treatment, highlighting the significance of such practice among patients with AGC.

## RESULTS

### Baseline characteristics and treatment outcomes in the retrospective exploratory and chemotherapy cohorts

Among the 253 patients in the retrospective exploratory and chemotherapy cohorts, 152 were treated with PD-1 inhibitors, while 101 were treated with irinotecan (Table 1). The median age was 57 years old, and there were more male patients (55.7%). Of the 152 patients treated with PD-1 inhibitors, 85 (55.9%) and 67 (44.1%) were treated with nivolumab and pembrolizumab, respectively. There were no differences in baseline clinicopathologic characteristics between patients treated with PD-1 inhibitors and those treated with irinotecan. The objective response rate and the disease control rate for the overall population were 7.1% and 37.5%, respectively, without any differences based on treatment. Similarly, progression-free survival (PFS) and overall survival (OS) were comparable in patients treated with PD-1 inhibitors and those treated with irinotecan (Figures S1A and S1B), although crossover of survival curves was commonly observed in both PFS and OS.

### Administration of pATBs and treatment outcomes in the retrospective exploratory and chemotherapy cohorts

Among the 152 patients treated with PD-1 inhibitors, 137 (90.1%) received ATBs between the initial diagnosis of AGC and administration of PD-1 inhibitors. To define the best cutoff value for the interval between the last ATB administration and ICI treatment to predict PFS, the log-rank maximization method was performed in patients of the retrospective exploratory cohort treated with PD-1 blockade. This analysis revealed that pATB administration within 28 days of treatment with PD-1 inhibitors most fairly predicted PFS. In contrast, an adequate cutoff value to associate the interval between last pATB administration and PFS with statistical significance could not be defined in patients treated with irinotecan. Based on this cutoff (28 days), 67 (44.1%) of 152 patients treated with PD-1 inhibitors and 41 (40.6%) of 101 patients treated with chemotherapy received ATBs within 28 days before the initiation of treatment (Table S1). There were no apparent differences in baseline characteristics between the pATB and non-pATB groups in the retrospective exploratory cohort (Table S2). When treatment responses were analyzed, the objective response rate (11.8% vs. 1.5%) and the disease control rate (52.9% vs. 16.4%) were significantly higher in the non-pATB group than in the pATB group (Table 2). In addition, pATB administration was associated with decreased PFS (hazard ratio [HR] = 2.897, 95% confidence interval [CI] = 2.043–4.109) and OS (HR = 2.294, 95% CI = 1.622–3.242) among patients treated with PD-1 inhibitors (Figures 2A and 2B). In contrast to the findings observed in patients treated with PD-1 inhibitors, treatment outcomes including response and survival did not differ according to pATB administration in patients treated with irinotecan (Table 2; Figures 2C and 2D). When the duration of pATB administration within 28 days of treatment initiation was computed, pATB duration of more than 3 days was most significantly associated with poor PFS and OS in patients treated with PD-1 blockade (Figures S2A and S2B). However,

**Table 1. Baseline characteristics of the retrospective exploratory cohort treated with anti-PD-1 and chemotherapy cohort treated with irinotecan**

	Total (N = 253)	Retrospective exploratory cohort (N = 152)	Chemotherapy cohort (N = 101)	p
Age				0.353 <sup>a</sup>
Median (range)	57 (20–88)	57 (29–91)	58 (20–86)	
Gender				0.223 <sup>b</sup>
Male (%)	141 (55.7)	80 (52.6)	61 (60.4)	
Female (%)	112 (44.3)	72 (47.4)	40 (39.6)	
Differentiation				0.204 <sup>b</sup> (0.194 <sup>c</sup> )
Well differentiated (%)	8 (3.2)	4 (2.6)	4 (4.0)	
Moderately differentiated (%)	78 (30.8)	40 (26.3)	38 (37.6)	
Poorly differentiated (%)	123 (48.6)	81 (53.3)	42 (41.6)	
Signet ring cell carcinoma (%)	44 (17.4)	27 (17.8)	17 (16.8)	
HER-2				0.615 <sup>b</sup>
Negative (%)	220 (87.3)	134 (88.2)	86 (86.0)	
Positive (%)	32 (12.7)	18 (11.8)	14 (14.0)	
Not assessed	1	0	1	
MSI/MMR				0.445 <sup>b</sup> (0.514 <sup>c</sup> )
MSS/pMMR (%)	229 (95.8)	142 (96.6)	87 (94.6)	
MSI-H/dMMR (%)	10 (4.2)	5 (3.4)	5 (5.4)	
Not assessed	14	5	9	
EBV				0.431 <sup>b</sup> (0.537 <sup>c</sup> )
Negative (%)	225 (95.3)	137 (94.5)	88 (96.7)	
Positive (%)	11 (4.7)	8 (5.5)	3 (3.3)	
Not assessed	17	7	10	
PD-L1 TPS				0.306 <sup>b</sup> (0.528 <sup>c</sup> )
TPS <1% (%)	121 (87.1)	95 (85.6)	26 (92.9)	
TPS ≥1% (%)	18 (12.9)	16 (14.4)	2 (7.1)	
Not assessed	114	41	73	
PD-L1 CPS				0.375 <sup>b</sup>
CPS <1 (%)	74 (53.2)	57 (51.4)	17 (60.7)	
CPS ≥1 (%)	65 (46.8)	54 (48.6)	11 (39.3)	
Not assessed	114	41	73	
Previous gastrectomy				0.700 <sup>b</sup>
No (%)	129 (51.0)	79 (52.0)	50 (49.5)	
Yes (%)	124 (49.0)	73 (48.0)	51 (50.5)	
Line of treatment				0.257 <sup>b</sup>
≤3 (%)	152 (60.1)	87 (57.2)	65 (64.4)	
≥4 (%)	101 (39.9)	65 (42.8)	36 (35.6)	
Prior antibiotics within 4 weeks				0.583 <sup>b</sup>
No (%)	145 (57.3)	85 (55.9)	60 (59.4)	
Yes (%)	108 (42.7)	67 (44.1)	41 (40.6)	

PD-1, programmed cell death protein-1; HER-2, human epidermal growth factor-2; MSI, microsatellite instability; MMR, mismatch repair; MSS, microsatellite stable; pMMR, mismatch repair proficient; MSI-H, microsatellite instability-high; dMMR, mismatch repair deficient; EBV, Epstein-Barr virus; PD-L1, programmed death-ligand 1; TPS, tumor proportion score; CPS, combined positive score.

<sup>a</sup>Unpaired t test.

<sup>b</sup>Chi-squared test.

<sup>c</sup>Fisher's exact test.

this phenomenon was similarly observed in patients treated with irinotecan (Figures S2C and S2D), revealing that the duration of pATB administration was not specifically associated with

the outcomes of PD-1 blockade or irinotecan treatment. In addition, the classes of pATBs were not significantly associated with survival outcome.

**Table 2. Treatment response of patients according to the administration of pATBs within 28 days of treatment initiation**

Patients treated with PD-1 inhibitors (retrospective exploratory cohort)				
	Total (N = 152)	pATBs (–) (N = 85)	pATBs (+) (N = 67)	p
Best response				<0.001 <sup>a,b</sup>
Complete response (%)	0 (0.0)	0 (0.0)	0 (0.0)	
Partial response (%)	11 (7.2)	10 (11.8)	1 (1.5)	
Stable disease (%)	45 (29.6)	35 (41.2)	10 (14.9)	
Progressive disease (%)	65 (42.8)	29 (34.1)	36 (53.7)	
Not assessed (%)	31 (20.4)	11 (12.9)	20 (29.9)	
Objective response rate (%)	11 (7.2)	10 (11.8)	1 (1.5)	0.034 <sup>a</sup> (0.049 <sup>c</sup> )
Disease control rate (%)	56 (36.8)	45 (52.9)	11 (16.4)	<0.001 <sup>a</sup>
Patients treated with irinotecan (chemotherapy cohort)				
	Total (N = 101)	pATBs (–) (N = 60)	pATBs (+) (N = 41)	p
Best response				0.096 <sup>a</sup> (0.085 <sup>b</sup> )
Complete response (%)	0 (0.0)	0 (0.0)	0 (0.0)	
Partial response (%)	7 (6.9)	5 (8.3)	2 (4.9)	
Stable disease (%)	32 (31.7)	21 (35.0)	11 (26.8)	
Progressive disease (%)	44 (43.6)	28 (46.7)	16 (39.0)	
Not assessed (%)	18 (17.8)	6 (10.0)	12 (29.3)	
Objective response rate (%)	7 (6.9)	5 (8.3)	2 (4.9)	0.712 <sup>a</sup> (1.000 <sup>c</sup> )
Disease control rate (%)	39 (38.6)	26 (43.3)	13 (31.7)	0.773 <sup>a</sup>
Patients treated with PD-1 inhibitors (retrospective validation cohort)				
	Total (N = 123)	pATBs (–) (N = 66)	pATBs (+) (N = 57)	p
Best response				<0.001 <sup>a,b</sup>
Complete response (%)	0 (0.0)	0 (0.0)	0 (0.0)	
Partial response (%)	8 (6.5)	8 (12.1)	0 (0.0)	
Stable disease (%)	48 (39.0)	38 (57.6)	10 (17.5)	
Progressive disease (%)	51 (41.5)	15 (22.7)	36 (63.2)	
Not assessed (%)	16 (13.0)	5 (7.6)	11 (19.3)	
Objective response rate (%)	8 (6.5)	8 (12.1)	0 (0.0)	0.011 <sup>a</sup> (0.010 <sup>c</sup> )
Disease control rate (%)	56 (45.5)	46 (69.7)	10 (17.5)	<0.001 <sup>a</sup>

pATBs, prior antibiotics; PD-1, programmed cell death protein-1.

<sup>a</sup>Chi-squared test.

<sup>b</sup>Mantel-Haenszel chi-squared test.

<sup>c</sup>Fisher's exact test.

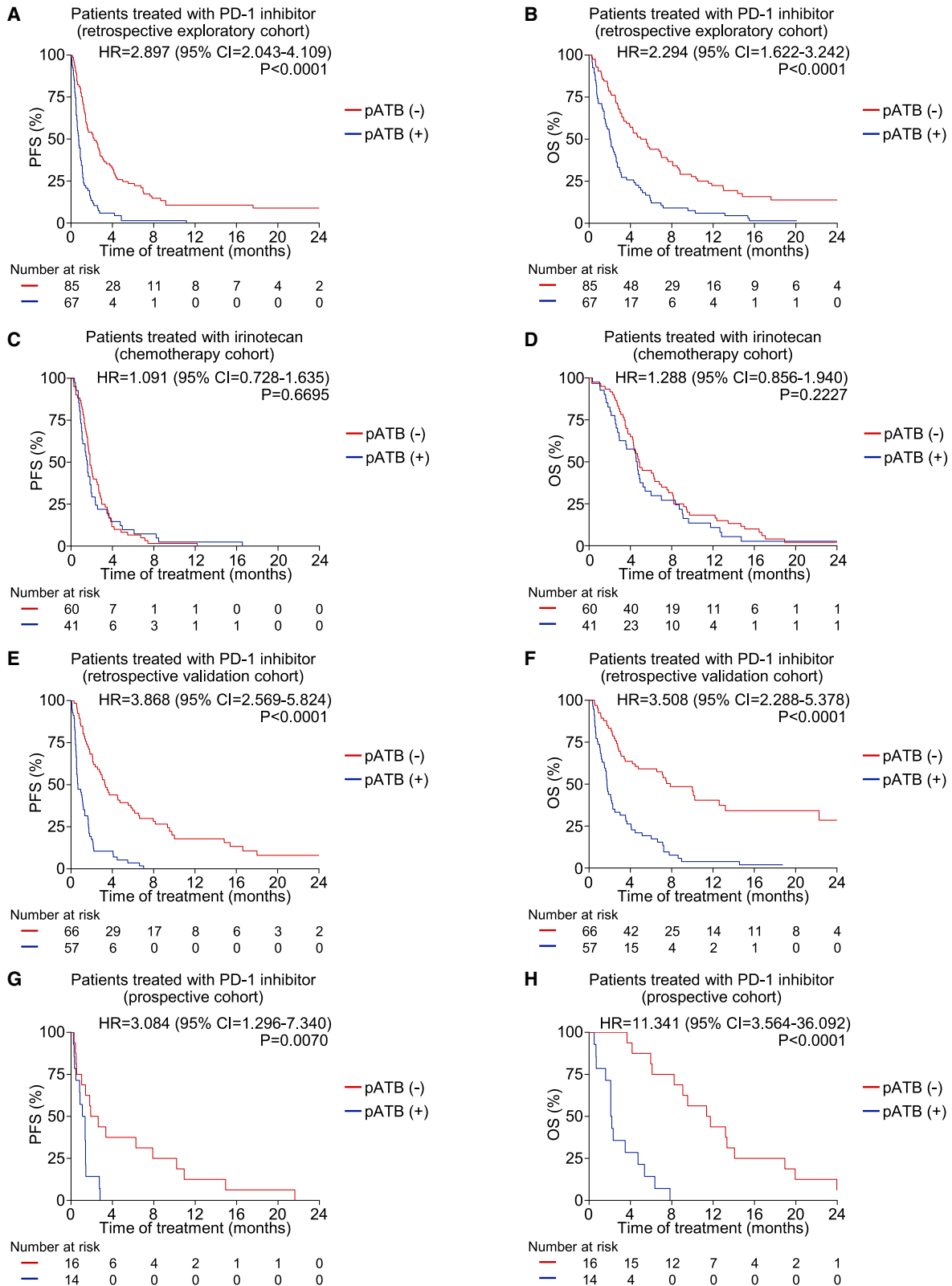
### Administration of pATBs and treatment outcomes in the retrospective and prospective validation cohorts

To validate the association between the efficacy of ICIs and pATB administration, we performed the same analysis in the retrospective validation cohort at another tertiary referral center. There were no differences in baseline characteristics between the retrospective exploratory and validation cohorts except in the line of treatment and administered drugs (Table S3). Outcomes following PD-1 treatment were comparable in the retrospective exploratory and validation cohorts. Compared with patients with pATB administration, those without pATB administration exhibited an increased likelihood of achieving objective response (12.1% vs. 0.0%) and disease control (69.7% vs. 17.5%) in the retrospective validation cohort (Table 2). Further, pATB administration was consistently associated with inferior PFS (HR = 3.868, 95% CI = 2.569–5.824) and OS (HR = 3.508, 95% CI = 2.288–5.378) after PD-1

inhibitor treatment (Figures 2E and 2F). To further validate these findings prospectively, we examined whether pATB administration was associated with survival outcomes in the prospective validation cohort composed of patients enrolled in clinical trials with pembrolizumab or nivolumab monotherapy (Table S4). Similar to the findings of the retrospective exploratory and validation cohorts (Figures 2A, 2B, 2E, and 2F), pATB administration was associated with poor PFS and OS (Figures 2G and 2H).

### Univariable and multivariable analyses among patients treated with PD-1 inhibitors

Univariable and multivariable analyses were performed to examine the associations between baseline characteristics and survival among all patients in the retrospective exploratory, retrospective validation, and prospective validation cohorts. Univariable analysis of all patients treated with PD-1 inhibitors



(legend on next page)



revealed that signet ring cell histology (HR = 1.417, 95% CI = 1.069–1.878), microsatellite stable/mismatch repair proficient tumor (HR = 2.525, 95% CI = 1.111–5.747),  $\geq 4$  lines of treatment (HR = 1.291, 95% CI = 1.008–1.652), and pATB administration (HR = 3.255, 95% CI = 2.529–4.191) were significantly associated with inferior PFS (Table 3).

On multivariable analysis, line of treatment (HR = 1.389, 95% CI = 1.055–1.829), and pATB administration (HR = 3.243, 95% CI = 2.427–4.333) were associated with inferior PFS. Similarly, pATB administration was independently associated with inferior OS (HR = 3.046, 95% CI = 2.358–3.935). When the analyses were performed separately based on the cohort, only pATB administration was commonly associated with both inferior PFS and OS in patients treated with PD-1 inhibitors in an independent manner (Tables S5–S7). Further, the association between pATB administration and survival outcomes was consistently observed irrespective of microsatellite instability/mismatch repair status or, Epstein-Barr virus status (Figures S3A–S3F;  $P_{\text{interaction}}$  for PFS = 0.157 and for OS = 0.850). There were 146 documentations of immune-related adverse events. The association between pATB administration and survival outcomes was consistently observed irrespective of the occurrence of immune-related adverse events during treatment (Figures S4A–S4F;  $P_{\text{interaction}}$  for PFS = 0.165 and for OS = 0.851). Administration of pATBs was not associated with the occurrence of immune-related adverse events.

### Effects of pATB administration on gut microbiota and circulating immune cells

To provide mechanistic insights into the association between pATB administration and worsened clinical outcomes, we analyzed fecal and blood samples obtained before administration of PD-1 inhibitors in patients with AGC (experimental stool/blood analysis cohort; Table S8). As in the other cohorts treated with PD-1 blockade, pATB administration was associated with inferior PFS and OS in the experimental stool/blood analysis cohort (Figures 3A and 3B; Table S9). To investigate whether the composition of gut microbiome was associated with pATB administration, we analyzed the fecal microbiota composition by 16S rRNA gene amplicon sequencing. Principal-coordinates analysis based on unweighted UniFrac distance indicated that pATB administration profoundly affected the overall composition of the gut microbiome (Figure 3C). The taxonomic alpha diversity based on Shannon index within each sample suggested that the diversity of the gut microbiome was significantly reduced by pATB administration (Figure 3D). In particular, the PFS and OS were significantly longer in patients with high Shannon index scores than those with low scores (Figures 3E and 3F). We found that 26 amplicon sequence variants had a significantly different relative abundance according to pATB administration (Figure 3G). Intriguingly, the relative

abundance of *Lactobacillus gasseri* was commonly associated with PFS and OS among those 26 amplicon sequence variants (Figure S5). Patients with a high relative abundance of *Lactobacillus gasseri* had significantly longer PFS and OS than those with its low abundance (Figures 3H and 3I).

Next, we performed scRNA-seq of circulating peripheral blood immune cells using the 10x Genomics platform and analyzed a total of 59,485 cells after filtering dead cells. Based on a uniform manifold approximation and projection (UMAP) algorithm (Figure 4A), we identified 11 different cell types using representative marker genes (Figures 4B and S6A). These clusters and annotated cell types were unbiased according to individual patients (Figure S6B). After excluding red blood cells, platelets, and undefined subsets, we focused on 10 cell types for further analysis. Subclustering analysis of mononuclear phagocytes (Figures 4C, S7A, and S7B) and natural killer (NK) and T lymphocytes (Figures 4D, S8A, and S8B) identified 6 and 13 distinct subclusters, respectively. When we compared the relative frequency of each subcluster (Figure 4E), the exhaustive CD8 T subcluster significantly expanded in patients administered with pATBs (Figure 4F). The exhaustive CD8 T subcluster was characterized by high expression of various immune checkpoint co-inhibitory receptors, such as *PDCD1*, *CTLA4*, *HAVCR2*, *LAG3*, and *TIGIT*, transcription factors related to T cell exhaustion including *TOX*, and genes associated with tissue-homing properties like *CD69* and *ITGAE* (Figure S9A). Correspondingly, a distinct transcriptional program was operated in the exhaustive CD8 T subcluster compared with the effector CD8 T or naive/central memory CD8 T subclusters (Figures S9B–S9D). Next, we analyzed the correlation between relative frequency of each cluster and clinical outcome. We identified robust correlation between the frequency of the exhaustive CD8 T cluster and the effector CD8 T cluster in the whole patient group (Figures S9E–S9H). Survival analysis revealed that disproportional expansion of the exhaustive CD8 T cluster compared with the effector CD8 T cluster was significantly associated with a poor clinical outcome (Figures 4G and 4H). The diversity of the T cell receptor repertoire was not associated with pATB administration or outcomes (Figures S10A–S10J). Collectively, our translational analysis provided mechanistic evidence that pATB administration induces microbial dysbiosis and altered systemic immune responses, contributing to the detrimental outcome of PD-1 blockade in AGC upon pATB exposure.

## DISCUSSION

In this study, we investigated the association between pATB administration and outcomes following PD-1 blockade or irinotecan chemotherapy in patients with AGC. While our findings indicated that pATB administration was associated with poor outcomes following PD-1 inhibitor treatment, no such association was observed in patients treated with irinotecan, a cytotoxic

### Figure 2. Survival outcomes according to the administration of pATBs within 28 days prior to the start of treatment

(A and B) PFS (A) and OS (B) in the retrospective exploratory cohort treated with PD-1 inhibitors according to the administration of pATBs.

(C and D) PFS (C) and OS (D) in the chemotherapy cohort treated with irinotecan according to the administration of pATBs.

(E and F) PFS (E) and OS (F) in the retrospective validation cohort treated with PD-1 inhibitors according to the administration of pATBs.

(G and H) PFS (G) and OS (H) in the prospective validation cohort treated with PD-1 inhibitors according to the administration of pATBs.

PD-1, programmed death-1; HR, hazard ratio; CI, confidence interval; pATBs, prior antibiotics; PFS, progression-free survival; OS, overall survival.

**Table 3. Cox regression analysis for PFS and OS in patients treated with PD-1 inhibitors in the retrospective exploratory cohort, retrospective validation cohort, and prospective validation cohort**

	Analysis for PFS				Analysis for OS			
	Univariable analysis		Multivariable analysis		Univariable analysis		Multivariable analysis	
	HR (95% CI)	p	HR (95% CI)	p	HR (95% CI)	p	HR (95% CI)	p
Age		0.134				0.088		
<65 years old	reference		–		reference		–	
≥65 years old	0.806 (0.609–1.069)		–		0.772 (0.573–1.040)		–	
Gender		0.195				0.354		
Female	reference		–		reference		–	
Male	0.858 (0.680–1.082)		–		0.891 (0.698–1.137)		–	
Differentiation		0.015		0.195		0.075		
Non-SRC	reference		reference		reference		–	
SRC	1.417 (1.069–1.878)		1.236 (0.897–1.702)		1.312 (0.973–1.770)		–	
HER-2		0.985				0.525		
Negative	reference		–		reference		–	
Positive	0.996 (0.682–1.455)		–		0.880 (0.594–1.305)		–	
MSI/MMR		0.027		0.161		0.088		
MSS/pMMR	reference		reference		reference		–	
MSI-H/dMMR	0.396 (0.174–0.900)		0.550 (0.238–1.269)		0.491 (0.216–1.113)		–	
EBV		0.457				0.249		
Negative	reference		–		reference		–	
Positive	0.776 (0.398–1.514)		–		0.674 (0.344–1.319)		–	
PD-L1 TPS		0.541				0.759		
TPS <1%	reference		–		reference		–	
TPS ≥1%	1.152 (0.732–1.813)		–		1.076 (0.674–1.717)		–	
PD-L1 CPS		0.269				0.110		
CPS <1	reference		–		reference		–	
CPS ≥1	0.834 (0.605–1.150)		–		0.761 (0.544–1.064)		–	
Line of treatment		0.043		0.019		0.012		0.002
≤3	reference		reference		reference		reference	
≥4	1.291 (1.008–1.652)		1.389 (1.055–1.829)		1.387 (1.075–1.790)		1.509 (1.168–1.949)	
Drug		0.176				0.291		
Pembrolizumab	reference		–		reference		–	
Nivolumab	1.211 (0.918–1.597)		–		1.168 (0.875–1.559)		–	
pATBs		<0.001		<0.001		<0.001		<0.001
No	reference		reference		reference		reference	
Yes	3.255 (2.529–4.191)		3.243 (2.427–4.333)		2.952 (2.287–3.810)		3.046 (2.358–3.935)	

PFS, progression-free survival; OS, overall survival; PD-1, programmed cell death protein-1; HR, hazard ratio; CI, confidence interval; SRC, signet ring cell; HER-2, human epidermal growth factor-2; MSI, microsatellite instability; MMR, mismatch repair; MSS, microsatellite stable; pMMR, mismatch repair proficient; MSI-H, microsatellite instability-high; dMMR, mismatch repair deficient; EBV, Epstein-Barr virus; PD-L1, programmed death-ligand 1; TPS, tumor proportion score; CPS, combined positive score, pATBs, prior antibiotics within 28 days.

chemotherapeutic agent. The association between pATB administration and outcomes of PD-1 blockade was further validated in other independent retrospective and prospective cohorts of patients treated with PD-1 inhibitors. When patients in these cohorts were considered, pATB administration was associated with reduced response rate and impaired survival in terms of both PFS and OS, suggesting that pATB administration represents a therapeutically actionable target for patients planning to undergo treatment with PD-1 inhibitors. Analysis of gut microbiome and circulating immune cells revealed distinct features

associated with administration of pATBs, supporting a mechanistic link between pATB administration and worsened clinical outcomes in patients treated with PD-1 blockade.

Several hypotheses can be suggested to associate pATB administration and treatment outcomes of PD-1 blockade. Pharmacokinetic or pharmacomicrobiomic interactions between anti-PD-1 antibody and ATBs would influence the outcome of PD-1 blockade.<sup>24,25</sup> In addition, preclinical and clinical studies have reported that imbalances in the microflora induced by ATB administration may negatively impact the outcomes of



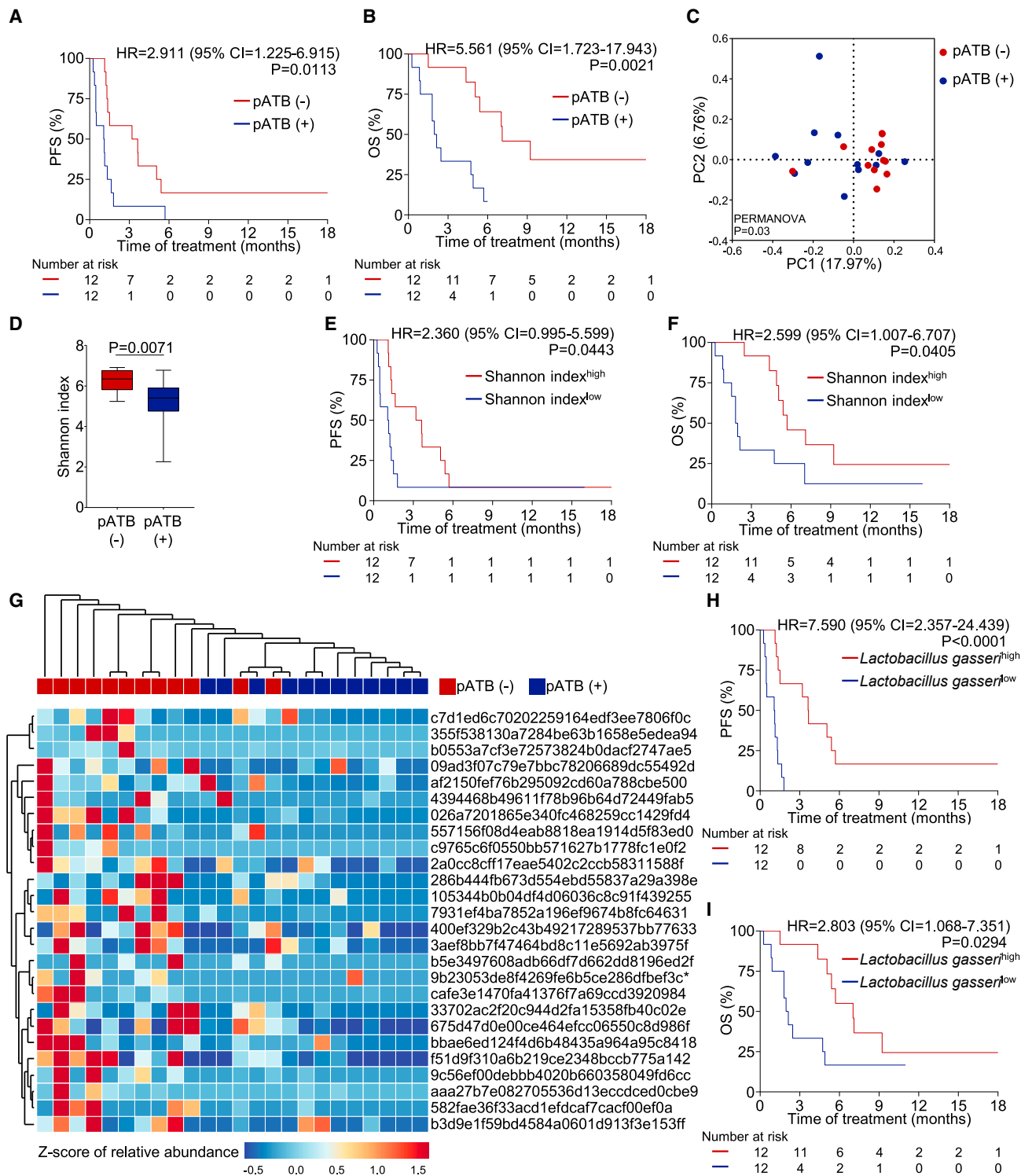


**Figure 3. Comparison of gut microbiome composition according to the administration of pATBs within 28 days prior to the start of treatment** (A and B) PFS (A) and OS (B) in the experimental stool/blood analysis cohort treated with PD-1 inhibitors according to the administration of pATBs. (C) PC analysis of gut microbiota based on unweighted UniFrac distances. PERMANOVA was performed to compare the differences of gut microbial community according to the administration of pATBs. (D) Diversity of gut microbiota based on Shannon index according to the administration of pATBs.

(legend continued on next page)

immune checkpoint blockade.<sup>26</sup> However, few studies have explored whether pATB administration is associated with alterations in gut microbiome, systemic immune responses, and outcomes of PD-1 blockade in patients with AGC, especially in relation to other treatment modalities. This study provides evidence that pATB administration worsens outcomes among patients with AGC receiving PD-1 inhibitors with translational analysis, underscoring the importance of microbiota homeostasis and systemic immune responses in determining the treatment response to immune checkpoint blockade.

Currently, several factors have been known to be associated with outcomes following PD-1 inhibitor treatment in patients with AGC, including PD-L1 expression,<sup>5,27</sup> microsatellite instability or mismatch repair deficiency status,<sup>5,27</sup> tumor mutation burden,<sup>28</sup> Epstein-Barr virus infection,<sup>10</sup> and gene expression profile.<sup>5,29</sup> In addition to tumor-intrinsic factors or microenvironment-derived immune signatures,<sup>30–32</sup> researchers have suggested that the cancer microbiome exerts a profound influence on the efficacy of immune checkpoint blockade.<sup>33</sup> Although preclinical studies have provided ample evidence,<sup>34</sup> human studies have also suggested that the microbiome can determine the response to treatment with PD-1 inhibitors, based on the finding that fecal microbiota transplantation can overcome resistance to immunotherapy.<sup>35,36</sup> In these two first-in-human studies,<sup>35,36</sup> patients who were previously refractory to ICIs underwent fecal microbiota transplantation using stool collected from patients with complete or partial response to immune checkpoint blockade, following which they were treated with PD-1 blockade. Strikingly, objective response was achieved in approximately a quarter of the analyzed patients, suggesting that altering the gut microbiome can reprogram the tumor microenvironment and improve the therapeutic efficacy of PD-1 inhibitors. Our study directly demonstrated that pATB administration reduced the diversity of gut microbiota, resulting in worsened outcomes in patients with AGC treated with PD-1 blockade. Furthermore, the relative abundance of *Lactobacillus gasseri* was significantly diminished by pATB administration and associated with the outcome of PD-1 inhibitors. Previously, the abundance of *Lactobacillus gasseri* was negatively associated with LAG3 expression,<sup>37</sup> an immune checkpoint co-inhibitory receptor imposing anti-PD-1 resistance.<sup>38,39</sup> In addition, recent studies identified that *Lactobacillus gasseri* treatment reduced the production of proinflammatory cytokines,<sup>40</sup> which can be translated to enhanced anti-PD-1 response. The differences in the composition of circulating T lymphocytes according to pATB administration is similar to previous findings, which demonstrated dysregulation of T cell immunity following exposure to ATBs.<sup>41,42</sup>

Our study uncovered that pATB administration was associated with enrichment of exhausted CD8<sup>+</sup> T cells expressing multiple immune checkpoint co-inhibitory receptors. Intriguingly, exhausted CD8<sup>+</sup> T cells highly expressed *PDCD1* and *EOMES* but expressed *TCF7* and *TBX21* less, suggesting the terminal differentiation status of this subset. The *EOMES*<sup>hi</sup>T-bet<sup>lo</sup>PD-1<sup>hi</sup> terminal progeny subset is less likely to be reinvigorated by PD-1 blockade,<sup>43</sup> associated with anti-PD-1 resistance. In line with this, a balance between the exhausted CD8 T and effector CD8 T subsets was associated with clinical outcomes of patients with AGC treated with PD-1 blockade in our study. Collectively, comparison of the single-cell landscape of circulating immune cells in patients with AGC treated with PD-1 blockade demonstrated a predictive value for disturbances in T cell differentiation and fate decision following pATB administration.

Prescription of ATBs is occasionally performed during the treatment course of AGC to deal with various clinical scenarios.<sup>23</sup> Anatomic characteristics of AGC, such as frequent involvement of the peritoneum leading to bowel obstruction, biliary tract involvement leading to biliary sepsis, and urinary tract involvement leading to urinary tract infection, contribute to the high rate of ATB usage.<sup>44</sup> In addition, cytotoxic chemotherapy forms the basis of earlier treatment for AGC, resulting in immune suppression and an increased risk of infection. Accordingly, 45.6% (150/329) of patients in our study treated with PD-1 inhibitors received pATBs within 28 days of treatment initiation, which is higher than the rate reported for other types of cancer.<sup>21,22</sup> Our findings suggest that clinicians should be cautious when prescribing ATB treatment prior to PD-1 blockade, based on preclinical and clinical evidence that dysbiosis of the microbiome and alteration of systemic immune response is common following ATB treatment. Considering that the objective response to PD-1 blockade in patients with AGC is modest when compared with that observed in patients with other types of cancer, our findings may help to identify subgroups of patients who are more likely to benefit from PD-1 inhibitor treatment or aid future researchers in enhancing the therapeutic efficacy of PD-1 inhibitors. Hence, future studies should aim to investigate whether therapeutic interventions with the administration of pATBs could improve outcomes following PD-1 blockade in patients with AGC. In addition, whether pATB administration is associated with outcome in patients treated with immune checkpoint blockade combined with chemotherapy would also be an intriguing area of future research, based on the established role of PD-1 inhibitor plus chemotherapy in first line setting.<sup>45</sup>

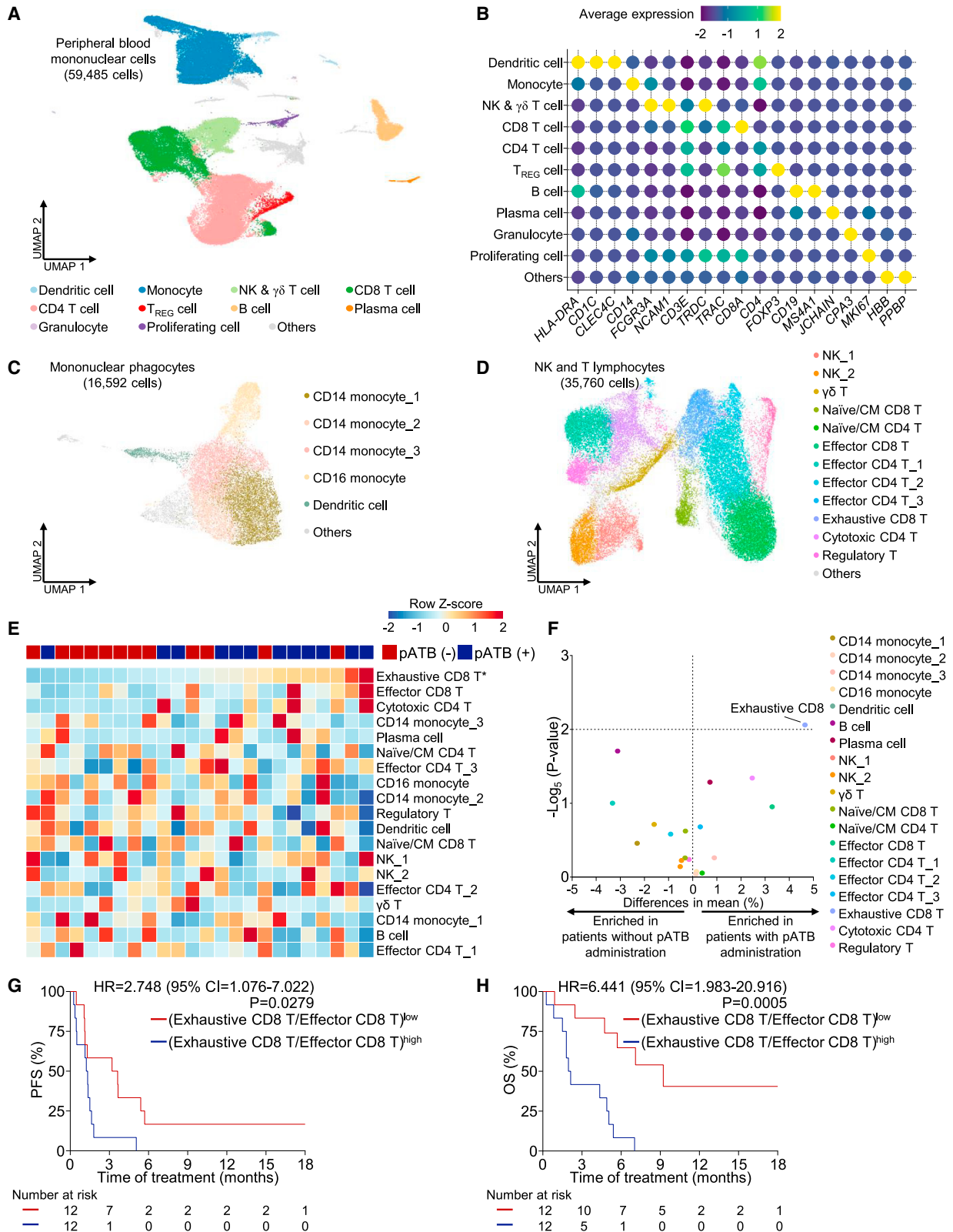
In summary, our findings indicate that administration of pATBs is specifically associated with inferior outcomes following PD-1

(E and F) PFS (E) and OS (F) according to the diversity of gut microbiota based on Shannon index. The median Shannon index value was used to define the “Shannon index<sup>high</sup>” and “Shannon index<sup>low</sup>” subgroups.

(G) Heatmap showing the significantly different 26 amplicon sequence variants according to the administration of pATBs. The heatmap was constructed by hierarchical clustering using the unweighted pair group method with an arithmetic mean. The color pattern on heatmap represents column Z score. Asterisks indicate amplicon sequence variants with survival implication (*Lactobacillus gasseri*).

(H and I) PFS (H) and OS (I) according to the abundance of *Lactobacillus gasseri*. The median abundance of *Lactobacillus gasseri* was used to define the “*Lactobacillus gasseri*<sup>high</sup>” and “*Lactobacillus gasseri*<sup>low</sup>” subgroups.

HR, hazard ratio; CI, confidence interval; pATBs, prior antibiotics; PFS, progression-free survival; OS, overall survival; PC, principal coordinate; PERMANOVA, permutational multivariate analysis of variance; PD-1, programmed death-1.



(legend on next page)

inhibitor treatment in patients with AGC but not following irinotecan chemotherapy. Mechanistically, pATB administration alters gut microbiota and systemic immune responses, thereby hindering the efficacy of PD-1 blockade. Further large prospective studies accompanied by translational analysis would confirm the findings of our study. In addition, whether therapeutic intervention regarding prescription of pATBs or transplantation of specific commensal bacteria alters the treatment outcomes of PD-1 blockade would be another intriguing aspect for future studies. Further, investigating whether similar findings can be obtained in patients treated with combined ICIs and chemotherapy in patients with AGC could have a potential impact on future practice.

### Limitation of the study

Due to the retrospective nature of the retrospective exploratory cohort ( $n = 152$ ), the retrospective validation cohort ( $n = 123$ ), and the chemotherapy cohort ( $n = 101$ ), we could not completely exclude the possibility that patients with pATB administration had poorer performance status or other comorbidities compared with those without pATB administration. Future prospective studies adjusting for variables associated with patient performance status and comorbidities are warranted. In addition, most patients included in this study started PD-1 blockade before the COVID-19 pandemic, limiting our analysis regarding the association between COVID-19 infection and/or vaccination and the outcome of treatment with PD-1 inhibitors.

### STAR★METHODS

Detailed methods are provided in the online version of this paper and include the following:

- KEY RESOURCES TABLE
- RESOURCE AVAILABILITY
  - Lead contact
  - Materials availability
  - Data and code availability
- EXPERIMENTAL MODEL AND SUBJECT DETAILS
  - Patients
  - Follow-up and response evaluation
- METHOD DETAILS
  - Evaluation of tumor tissue
  - 16S ribosomal RNA sequencing with stool samples
  - scRNA-seq with circulating immune cells
- QUANTIFICATION AND STATISTICAL ANALYSIS

### SUPPLEMENTAL INFORMATION

Supplemental information can be found online at <https://doi.org/10.1016/j.xcrm.2023.101251>.

### ACKNOWLEDGMENTS

We express our sincere thanks to Yun Jin Choi, Jin Young Oh, and Ha Na Kwon (Songdang Institute for Cancer Research, Yonsei University College of Medicine, Seoul, Republic of Korea) for acquiring the data and Medical Illustration & Design, part of the Medical Research Support Services of Yonsei University College of Medicine, for artistic support related to this work. This work was supported by a National Research Foundation of Korea grant funded by the Korean government (2021R1A2C2009400 to M.J., 2022R1C1C1012634 to J.S.L., and 2021R1I1A1A01059271 to C.G.K.); the Main Research Program of the Korea Food Research Institute funded by the Ministry of Science and ICT (E0170600-06 to Y.-D.N.); a faculty research grant from the Yonsei University College of Medicine (6-2020-0231 to M.J.); and the Young Medical Scientist Research Grant Program of the Daewoong Foundation (DY20206P to C.G.K.).

### AUTHOR CONTRIBUTIONS

All authors meet authorship requirements. C.G.K., J.-Y.K., S.-J.S., J.-H.S., H.-C.J., J.S.L., Y.-D.N., and M.J. conceived and designed the study and take responsibility for the integrity of the data and preparation of manuscript. C.G.K., M.H., H.C.C., S.Y.R., H.S.K., C.-K.L., J.H.L., Y.H., Hyunki Kim, J.H.K., S.Y.L., S.K.P., S.P., Hyunwook Kim, J.Y.A., H.-C.J., and M.J. contributed to collection and analysis of the clinical data. C.G.K., J.-Y.K., J.S.L., Hyoyong Kim, X.C., U.-J.Y., and M.J. performed circulating immune cell analysis. C.G.K., J.-H.S., Hyoyong Kim, X.C., U.-J.Y., Y.-D.N., and M.J. performed microbiome analysis. C.G.K., J.-Y.K., S.-J.S., J.-H.S., H.-C.J., J.S.L., Y.-D.N., and M.J. wrote the first manuscript draft. All authors reviewed, revised, edited, and approved the final version of the manuscript.

### DECLARATION OF INTERESTS

The authors declare no competing interests.

Received: November 11, 2022

Revised: April 13, 2023

Accepted: September 27, 2023

Published: October 26, 2023

### REFERENCES

1. Xin Yu, J., Hubbard-Lucey, V.M., and Tang, J. (2019). Immuno-oncology drug development goes global. *Nat. Rev. Drug Discov.* 18, 899–900. <https://doi.org/10.1038/d41573-019-00167-9>.
2. Ribas, A., and Wolchok, J.D. (2018). Cancer immunotherapy using checkpoint blockade. *Science* 359, 1350–1355. <https://doi.org/10.1126/science.aar4060>.

### Figure 4. Single-cell transcriptomes of circulating immune cells from 24 patients treated with PD-1 blockade

- (A) UMAP of total 59,485 cells from peripheral blood, colored to show annotated cell types.
  - (B) Thirteen different cell types and their specific marker gene expression levels, where brightness indicates log-normalized average expression.
  - (C) UMAP of 16,592 mononuclear phagocytes from peripheral blood, colored to show annotated cell types.
  - (D) UMAP of 35,760 NK and T lymphocytes from peripheral blood, colored to show annotated cell types.
  - (E) The heatmap showing the relative abundance of each subclusters. Color pattern on heatmap represents column Z score. Asterisks indicate subclusters with survival implication (exhaustive CD8 T).
  - (F) Dot plot showing the differences of each subclusters and statistical significance according to the administration of pATBs.
  - (G and H) PFS (G) and OS (H) according to the ratio between exhaustive CD8 T and effector CD8 T subclusters. The median value of the ratio between exhaustive CD8 T and effector CD8 T subclusters was used to define the “(exhaustive CD8 T/effector CD8 T)<sup>high</sup>” and “(exhaustive CD8 T/effector CD8 T)<sup>low</sup>” subgroups.
- UMAP, uniform manifold approximation and projection; pATBs, prior antibiotics; HR, hazard ratio; CI, confidence interval; PFS, progression-free survival; OS, overall survival.



- Sharma, P., and Allison, J.P. (2020). Dissecting the mechanisms of immune checkpoint therapy. *Nat. Rev. Immunol.* 20, 75–76. <https://doi.org/10.1038/s41577-020-0275-8>.
- Waldman, A.D., Fritz, J.M., and Lenardo, M.J. (2020). A guide to cancer immunotherapy: from T cell basic science to clinical practice. *Nat. Rev. Immunol.* 20, 651–668. <https://doi.org/10.1038/s41577-020-0306-5>.
- Fuchs, C.S., Doi, T., Jang, R.W., Muro, K., Satoh, T., Machado, M., Sun, W., Jalal, S.I., Shah, M.A., Metges, J.P., et al. (2018). Safety and Efficacy of Pembrolizumab Monotherapy in Patients With Previously Treated Advanced Gastric and Gastroesophageal Junction Cancer: Phase 2 Clinical KEYNOTE-059 Trial. *JAMA Oncol.* 4, e180013. <https://doi.org/10.1001/jamaoncol.2018.0013>.
- Kang, Y.K., Boku, N., Satoh, T., Ryu, M.H., Chao, Y., Kato, K., Chung, H.C., Chen, J.S., Muro, K., Kang, W.K., et al. (2017). Nivolumab in patients with advanced gastric or gastro-oesophageal junction cancer refractory to, or intolerant of, at least two previous chemotherapy regimens (ONO-4538-12, ATTRACTION-2): a randomised, double-blind, placebo-controlled, phase 3 trial. *Lancet (London, England)* 390, 2461–2471. [https://doi.org/10.1016/s0140-6736\(17\)31827-5](https://doi.org/10.1016/s0140-6736(17)31827-5).
- Smyth, E.C., Nilsson, M., Grabsch, H.I., van Grieken, N.C., and Lordick, F. (2020). Gastric cancer. *Lancet* 396, 635–648. [https://doi.org/10.1016/s0140-6736\(20\)31288-5](https://doi.org/10.1016/s0140-6736(20)31288-5).
- Sung, H., Ferlay, J., Siegel, R.L., Laversanne, M., Soerjomataram, I., Jemal, A., and Bray, F. (2021). Global cancer statistics 2020: GLOBOCAN estimates of incidence and mortality worldwide for 36 cancers in 185 countries. *CA A Cancer J. Clin.* 71, 209–249. <https://doi.org/10.3322/caac.21660>.
- Kono, K., Nakajima, S., and Mimura, K. (2020). Current status of immune checkpoint inhibitors for gastric cancer. *Gastric Cancer* 23, 565–578. <https://doi.org/10.1007/s10120-020-01090-4>.
- Kim, S.T., Cristescu, R., Bass, A.J., Kim, K.M., Odegaard, J.I., Kim, K., Liu, X.Q., Sher, X., Jung, H., Lee, M., et al. (2018). Comprehensive molecular characterization of clinical responses to PD-1 inhibition in metastatic gastric cancer. *Nat. Med.* 24, 1449–1458. <https://doi.org/10.1038/s41591-018-0101-z>.
- Samstein, R.M., Lee, C.H., Shoushtari, A.N., Hellmann, M.D., Shen, R., Janjigian, Y.Y., Barron, D.A., Zehir, A., Jordan, E.J., Omuro, A., et al. (2019). Tumor mutational load predicts survival after immunotherapy across multiple cancer types. *Nat. Genet.* 51, 202–206. <https://doi.org/10.1038/s41588-018-0312-8>.
- Kim, C.G., Jang, M., Kim, Y., Leem, G., Kim, K.H., Lee, H., Kim, T.S., Choi, S.J., Kim, H.D., Han, J.W., et al. (2019). VEGF-A drives TOX-dependent T cell exhaustion in anti-PD-1-resistant microsatellite stable colorectal cancers. *Sci. Immunol.* 4, eaay0555. <https://doi.org/10.1126/sciimmunol.aay0555>.
- Kallies, A., Zehn, D., and Utzschneider, D.T. (2020). Precursor exhausted T cells: key to successful immunotherapy? *Nat. Rev. Immunol.* 20, 128–136. <https://doi.org/10.1038/s41577-019-0223-7>.
- Jhunjunwala, S., Hammer, C., and Delamarre, L. (2021). Antigen presentation in cancer: insights into tumour immunogenicity and immune evasion. *Nat. Rev. Cancer* 21, 298–312. <https://doi.org/10.1038/s41568-021-00339-z>.
- Sivan, A., Corrales, L., Hubert, N., Williams, J.B., Aquino-Michaels, K., Earley, Z.M., Benyamin, F.W., Lei, Y.M., Jabri, B., Alegre, M.L., et al. (2015). Commensal *Bifidobacterium* promotes antitumor immunity and facilitates anti-PD-L1 efficacy. *Science (New York, N.Y.)* 350, 1084–1089. <https://doi.org/10.1126/science.aac4255>.
- Vétizou, M., Pitt, J.M., Daillère, R., Lepage, P., Waldschmitt, N., Flament, C., Rusakiewicz, S., Routy, B., Roberti, M.P., Duong, C.P.M., et al. (2015). Anticancer immunotherapy by CTLA-4 blockade relies on the gut microbiota. *Science (New York, N.Y.)* 350, 1079–1084. <https://doi.org/10.1126/science.aad1329>.
- Routy, B., Le Chatelier, E., Derosa, L., Duong, C.P.M., Alou, M.T., Daillère, R., Fluckiger, A., Messaoudene, M., Rauber, C., Roberti, M.P., et al. (2018). Gut microbiome influences efficacy of PD-1-based immunotherapy against epithelial tumors. *Science* 359, 91–97. <https://doi.org/10.1126/science.aan3706>.
- Gopalakrishnan, V., Spencer, C.N., Nezi, L., Reuben, A., Andrews, M.C., Karpinets, T.V., Prieto, P.A., Vicente, D., Hoffman, K., Wei, S.C., et al. (2018). Gut microbiome modulates response to anti-PD-1 immunotherapy in melanoma patients. *Science* 359, 97–103. <https://doi.org/10.1126/science.aan4236>.
- Matson, V., Fessler, J., Bao, R., Chongsawat, T., Zha, Y., Alegre, M.L., Luke, J.J., and Gajewski, T.F. (2018). The commensal microbiome is associated with anti-PD-1 efficacy in metastatic melanoma patients. *Science* 359, 104–108. <https://doi.org/10.1126/science.aao3290>.
- Derosa, L., Routy, B., Desilets, A., Daillère, R., Terrisse, S., Kroemer, G., and Zitvogel, L. (2021). Microbiota-Centered Interventions: The Next Breakthrough in Immuno-Oncology? *Cancer Discov.* 11, 2396–2412. <https://doi.org/10.1158/2159-8290.CD-21-0236>.
- Derosa, L., Hellmann, M.D., Spaziano, M., Halpenny, D., Fidelle, M., Rizvi, H., Long, N., Plodkowski, A.J., Arbour, K.C., Chaff, J.E., et al. (2018). Negative association of antibiotics on clinical activity of immune checkpoint inhibitors in patients with advanced renal cell and non-small-cell lung cancer. *Ann. Oncol.* 29, 1437–1444. <https://doi.org/10.1093/annonc/mdl103>.
- Pinato, D.J., Howlett, S., Ottaviani, D., Urus, H., Patel, A., Mineo, T., Brock, C., Power, D., Hatcher, O., Falconer, A., et al. (2019). Association of Prior Antibiotic Treatment With Survival and Response to Immune Checkpoint Inhibitor Therapy in Patients With Cancer. *JAMA Oncol.* 5, 1774–1778. <https://doi.org/10.1001/jamaoncol.2019.2785>.
- Grealy, M., Chou, J.F., Chatila, W.K., Margolis, M., Capanu, M., Hechtman, J.F., Tuvy, Y., Kundra, R., Daian, F., Ladanyi, M., et al. (2019). Clinical and Molecular Predictors of Response to Immune Checkpoint Inhibitors in Patients with Advanced Esophagogastric Cancer. *Clin. Cancer Res.* 25, 6160–6169. <https://doi.org/10.1158/1078-0432.Ccr-18-3603>.
- Cortellini, A., Tucci, M., Adamo, V., Stucci, L.S., Russo, A., Tanda, E.T., Spagnolo, F., Rastelli, F., Bissoni, R., Santini, D., et al. (2020). Integrated analysis of concomitant medications and oncological outcomes from PD-1/PD-L1 checkpoint inhibitors in clinical practice. *J. Immunother. Cancer* 8, e001361. <https://doi.org/10.1136/jitc-2020-001361>.
- Ting, N.L.N., Lau, H.C.H., and Yu, J. (2022). Cancer pharmacomicrobiomics: targeting microbiota to optimise cancer therapy outcomes. *Gut* 71, 1412–1425. <https://doi.org/10.1136/gutjnl-2021-326264>.
- Gopalakrishnan, V., Helmink, B.A., Spencer, C.N., Reuben, A., and Wargo, J.A. (2018). The Influence of the Gut Microbiome on Cancer, Immunity, and Cancer Immunotherapy. *Cancer Cell* 33, 570–580. <https://doi.org/10.1016/j.ccell.2018.03.015>.
- Shitara, K., Özgüroğlu, M., Bang, Y.J., Di Bartolomeo, M., Mandalà, M., Ryu, M.H., Fornaro, L., Olesiński, T., Caglevic, C., Chung, H.C., et al. (2018). Pembrolizumab versus paclitaxel for previously treated, advanced gastric or gastro-oesophageal junction cancer (KEYNOTE-061): a randomised, open-label, controlled, phase 3 trial. *Lancet (London, England)* 392, 123–133. [https://doi.org/10.1016/s0140-6736\(18\)31257-1](https://doi.org/10.1016/s0140-6736(18)31257-1).
- Wang, F., Wei, X.L., Wang, F.H., Xu, N., Shen, L., Dai, G.H., Yuan, X.L., Chen, Y., Yang, S.J., Shi, J.H., et al. (2019). Safety, efficacy and tumor mutational burden as a biomarker of overall survival benefit in chemo-refractory gastric cancer treated with toripalimab, a PD-1 antibody in phase Ib/II clinical trial NCT02915432. *Ann. Oncol.* 30, 1479–1486. <https://doi.org/10.1093/annonc/mdz197>.
- Muro, K., Chung, H.C., Shankaran, V., Geva, R., Catenacci, D., Gupta, S., Eder, J.P., Golan, T., Le, D.T., Burtneis, B., et al. (2016). Pembrolizumab



- for patients with PD-L1-positive advanced gastric cancer (KEYNOTE-012): a multicentre, open-label, phase 1b trial. *Lancet Oncol.* 17, 717–726. [https://doi.org/10.1016/s1470-2045\(16\)00175-3](https://doi.org/10.1016/s1470-2045(16)00175-3).
30. Kalbasi, A., and Ribas, A. (2020). Tumour-intrinsic resistance to immune checkpoint blockade. *Nat. Rev. Immunol.* 20, 25–39. <https://doi.org/10.1038/s41577-019-0218-4>.
31. Bruni, D., Angell, H.K., and Galon, J. (2020). The immune contexture and Immunoscore in cancer prognosis and therapeutic efficacy. *Nat. Rev. Cancer* 20, 662–680. <https://doi.org/10.1038/s41568-020-0285-7>.
32. Ayers, M., Luceford, J., Nebozhyn, M., Murphy, E., Loboda, A., Kaufman, D.R., Albright, A., Cheng, J.D., Kang, S.P., Shankaran, V., et al. (2017). IFN- $\gamma$ -related mRNA profile predicts clinical response to PD-1 blockade. *J. Clin. Invest.* 127, 2930–2940. <https://doi.org/10.1172/jci91190>.
33. Elinav, E., Garrett, W.S., Trinchieri, G., and Wargo, J. (2019). The cancer microbiome. *Nat. Rev. Cancer* 19, 371–376. <https://doi.org/10.1038/s41568-019-0155-3>.
34. Mager, L.F., Burkhard, R., Pett, N., Cooke, N.C.A., Brown, K., Ramay, H., Paik, S., Stagg, J., Groves, R.A., Gallo, M., et al. (2020). Microbiome-derived inosine modulates response to checkpoint inhibitor immunotherapy. *Science (New York, N.Y.)* 369, 1481–1489. <https://doi.org/10.1126/science.abc3421>.
35. Baruch, E.N., Youngster, I., Ben-Betzalel, G., Ortenberg, R., Lahat, A., Katz, L., Adler, K., Dick-Necula, D., Raskin, S., Bloch, N., et al. (2021). Fecal microbiota transplant promotes response in immunotherapy-refractory melanoma patients. *Science (New York, N.Y.)* 371, 602–609. <https://doi.org/10.1126/science.abb5920>.
36. Davar, D., Dzusev, A.K., McCulloch, J.A., Rodrigues, R.R., Chauvin, J.M., Morrison, R.M., Deblasio, R.N., Menna, C., Ding, Q., Pagliano, O., et al. (2021). Fecal microbiota transplant overcomes resistance to anti-PD-1 therapy in melanoma patients. *Science (New York, N.Y.)* 371, 595–602. <https://doi.org/10.1126/science.abc3363>.
37. Łaniewski, P., Cui, H., Roe, D.J., Chase, D.M., and Herbst-Kralovetz, M.M. (2020). Vaginal microbiota, genital inflammation, and neoplasia impact immune checkpoint protein profiles in the cervicovaginal microenvironment. *npj Precis. Oncol.* 4, 22. <https://doi.org/10.1038/s41698-020-0126-x>.
38. Wang, J., Sanmamed, M.F., Datar, I., Su, T.T., Ji, L., Sun, J., Chen, L., Chen, Y., Zhu, G., Yin, W., et al. (2019). Fibrinogen-like Protein 1 Is a Major Immune Inhibitory Ligand of LAG-3. *Cell* 176, 334–347.e12. <https://doi.org/10.1016/j.cell.2018.11.010>.
39. Tawbi, H.A., Schadendorf, D., Lipson, E.J., Ascierto, P.A., Matamala, L., Castillo Gutiérrez, E., Rutkowski, P., Gogas, H.J., Lao, C.D., De Menezes, J.J., et al. (2022). Relatlimab and Nivolumab versus Nivolumab in Untreated Advanced Melanoma. *N. Engl. J. Med.* 386, 24–34. <https://doi.org/10.1056/NEJMoa2109970>.
40. Oh, N.S., Lee, J.Y., Kim, Y.T., Kim, S.H., and Lee, J.H. (2020). Cancer-protective effect of a synbiotic combination between *Lactobacillus gasseri* 505 and a *Cudrania tricuspidata* leaf extract on colitis-associated colorectal cancer. *Gut Microb.* 12, 1785803. <https://doi.org/10.1080/19490976.2020.1785803>.
41. Scott, N.A., Andrusaite, A., Andersen, P., Lawson, M., Alcon-Giner, C., Leclaire, C., Caim, S., Le Gall, G., Shaw, T., Connolly, J.P.R., et al. (2018). Antibiotics induce sustained dysregulation of intestinal T cell immunity by perturbing macrophage homeostasis. *Sci. Transl. Med.* 10, eaao4755. <https://doi.org/10.1126/scitranslmed.aao4755>.
42. He, Y., Fu, L., Li, Y., Wang, W., Gong, M., Zhang, J., Dong, X., Huang, J., Wang, Q., Mackay, C.R., et al. (2021). Gut microbial metabolites facilitate anticancer therapy efficacy by modulating cytotoxic CD8(+) T cell immunity. *Cell Metabol.* 33, 988–1000.e7. <https://doi.org/10.1016/j.cmet.2021.03.002>.
43. Pauken, K.E., and Wherry, E.J. (2015). Overcoming T cell exhaustion in infection and cancer. *Trends Immunol.* 36, 265–276. <https://doi.org/10.1016/j.it.2015.02.008>.
44. Li, W., Ng, J.M.K., Wong, C.C., Ng, E.K.W., and Yu, J. (2018). Molecular alterations of cancer cell and tumour microenvironment in metastatic gastric cancer. *Oncogene* 37, 4903–4920. <https://doi.org/10.1038/s41388-018-0341-x>.
45. Janjigian, Y.Y., Shitara, K., Moehler, M., Garrido, M., Salman, P., Shen, L., Wyrwicz, L., Yamaguchi, K., Skoczylas, T., Campos Bragagnoli, A., et al. (2021). First-line nivolumab plus chemotherapy versus chemotherapy alone for advanced gastric, gastro-oesophageal junction, and oesophageal adenocarcinoma (CheckMate 649): a randomised, open-label, phase 3 trial. *Lancet* 398, 27–40. [https://doi.org/10.1016/s0140-6736\(21\)00797-2](https://doi.org/10.1016/s0140-6736(21)00797-2).
46. Zheng, G.X., Terry, J.M., Belgrader, P., Ryvkin, P., Bent, Z.W., Wilson, R., Zivaldo, S.B., Wheeler, T.D., McDermott, G.P., Zhu, J., et al. (2017). Massively parallel digital transcriptional profiling of single cells. *Nat Commun* 8, 14049. <https://doi.org/10.1038/ncomms14049.55>.
47. Kang, H.M., Subramaniam, M., Targ, S., Nguyen, M., Maliskova, L., McCarthy, E., Wan, E., Wong, S., Byrnes, L., Lanata, C.M., et al. (2018). Multiplexed droplet single-cell RNA-sequencing using natural genetic variation. *Nat Biotechnol* 36, 89–94. <https://doi.org/10.1038/nbt.4042.56>.
48. Hafemeister, C., and Satija, R. (2019). Normalization and variance stabilization of single-cell RNA-seq data using regularized negative binomial regression. *Genome Biol* 20, 296. <https://doi.org/10.1186/s13059-019-1874-1.57>.
49. Chen, E.Y., Tan, C.M., Kou, Y., Duan, Q., Wang, Z., Meirelles, G.V., Clark, N.R., and Ma'ayan, A. (2013). Enrichr: interactive and collaborative HTML5 gene list enrichment analysis tool. *BMC Bioinformatics* 14, 128. <https://doi.org/10.1186/1471-2105-14-128.58>.
50. Subramanian, A., Tamayo, P., Mootha, V.K., Mukherjee, S., Ebert, B.L., Gillette, M.A., Paulovich, A., Pomeroy, S.L., Golub, T.R., Lander, E.S., and Mesirov, J.P. (2005). Gene set enrichment analysis: a knowledge-based approach for interpreting genome-wide expression profiles. *Proc Natl Acad Sci U S A* 102, 15545–15550. <https://doi.org/10.1073/pnas.0506580102.59>.
51. Robertson, A.G., Meghani, K., Cooley, L.F., McLaughlin, K.A., Fall, L.A., Yu, Y., Castro, M.A.A., Groeneveld, C.S., de Reyniès, A., Nazarov, V.I., et al. (2023). Expression-based subtypes define pathologic response to neoadjuvant immune-checkpoint inhibitors in muscle-invasive bladder cancer. *Nat Commun* 14, 2126. <https://doi.org/10.1038/s41467-023-37568-9>.
52. Bolyen, E., Rideout, J.R., Dillon, M.R., Bokulich, N.A., Abnet, C.C., Al-Ghathli, G.A., Alexander, H., Alm, E.J., Arumugam, M., Asnicar, F., et al. (2019). Reproducible, interactive, scalable and extensible microbiome data science using QIIME 2. *Nat. Biotechnol.* 37, 852–857. <https://doi.org/10.1038/s41587-019-0209-9>.
53. Eisenhauer, E.A., Therasse, P., Bogaerts, J., Schwartz, L.H., Sargent, D., Ford, R., Dancey, J., Arbuck, S., Gwyther, S., Mooney, M., et al. (2009). New Response Evaluation Criteria in Solid Tumours: Revised RECIST Guideline (Version 1.1), 45 (*European journal of cancer*), pp. 228–247. <https://doi.org/10.1016/j.ejca.2008.10.026>.
54. Lantuejoul, S., Sound-Tsao, M., Cooper, W.A., Girard, N., Hirsch, F.R., Roden, A.C., Lopez-Rios, F., Jain, D., Chou, T.Y., Motoi, N., et al. (2020). PD-L1 Testing for Lung Cancer in 2019: Perspective From the IASLC Pathology Committee. *J. Thorac. Oncol.* 15, 499–519. <https://doi.org/10.1016/j.jtho.2019.12.107>.
55. Park, J.S., Lee, N., Beom, S.H., Kim, H.S., Lee, C.K., Rha, S.Y., Chung, H.C., Yun, M., Cho, A., and Jung, M. (2018). The prognostic value of volume-based parameters using (18)F-FDG PET/CT in gastric cancer according to HER2 status. *Gastric Cancer* 21, 213–224. <https://doi.org/10.1007/s10120-017-0739-0>.

56. Kim, C.G., Ahn, J.B., Jung, M., Beom, S.H., Kim, C., Kim, J.H., Heo, S.J., Park, H.S., Kim, J.H., Kim, N.K., et al. (2016). Effects of microsatellite instability on recurrence patterns and outcomes in colorectal cancers. *Br. J. Cancer* *115*, 25–33. <https://doi.org/10.1038/bjc.2016.161>.
57. Callahan, B.J., McMurdie, P.J., Rosen, M.J., Han, A.W., Johnson, A.J.A., and Holmes, S.P. (2016). DADA2: High-resolution sample inference from Illumina amplicon data. *Nat. Methods* *13*, 581–583. <https://doi.org/10.1038/nmeth.3869>.
58. Rognes, T., Flouri, T., Nichols, B., Quince, C., and Mahé, F. (2016). VSEARCH: a versatile open source tool for metagenomics. *PeerJ* *4*, e2584. <https://doi.org/10.7717/peerj.2584>.
59. Lee, J.S., Park, S., Jeong, H.W., Ahn, J.Y., Choi, S.J., Lee, H., Choi, B., Nam, S.K., Sa, M., Kwon, J.S., et al. (2020). Immunophenotyping of COVID-19 and influenza highlights the role of type I interferons in development of severe COVID-19. *Sci. Immunol.* *5*, eabd1554. <https://doi.org/10.1126/sciimmunol.abd1554>.

**STAR★METHODS**

**KEY RESOURCES TABLE**

REAGENT or RESOURCE	SOURCE	IDENTIFIER
<b>Antibodies</b>		
Human epidermal growth factor receptor 2 (HER-2), clone GE001	Dako, Santa Clara, CA, USA,	HER-2, HercepTest™ Kit
MutL homolog 1 (MLH1), clone M1	Roche, Indianapolis, IN, USA,	Cat# 790-5091
MutS protein homolog 2 (MSH2), clone G219-1129	Roche, Indianapolis, IN, USA,	Cat# 790-5093
MutS homolog 6 (MSH6), clone 44	Cell Marque, Rocklin, CA, USA,	Cat#287M
Post-meiotic segregation increased 2 (PMS2), clone MRQ28	Cell Marque, Rocklin, CA, USA,	Cat#288M
Programmed death-ligand 1 (PD-L1), clone 22C3	Dako, Santa Clara, CA, USA,	PD-L1 IHC 22C3 pharmDx
<b>Biological samples</b>		
Stools from patients with advanced gastric cancer	This paper	N/A
Peripheral blood mononuclear cells from patients with advanced gastric cancer	This paper	N/A
<b>Critical commercial assays</b>		
Chromium Next GEM Single Cell 5' Kit v2	10x Genomics	PN-1000263
Chromium Single Cell Human TCR Amplification Kit	10x Genomics	PN-1000252
QIAamp DNA stool Mini kit (50 preps)	QIAGEN	<a href="https://www.qiagen.com/ko-us/products/discovery-and-translational-research/dna-rna-purification/dna-purification/genomic-dna/qiaamp-fast-dna-stool-mini-kit">https://www.qiagen.com/ko-us/products/discovery-and-translational-research/dna-rna-purification/dna-purification/genomic-dna/qiaamp-fast-dna-stool-mini-kit</a>
HER-2 silver <i>in situ</i> hybridisation, Ventana Benchmark ISH system and an ISH iView kit	Ventana Medical Systems, Tucson, AZ, USA	<a href="https://diagnostics.roche.com/global/en/products/tests/ventana-her2-dual-ish-dna-probe-cocktail-assay-fda.html">https://diagnostics.roche.com/global/en/products/tests/ventana-her2-dual-ish-dna-probe-cocktail-assay-fda.html</a>
EBV-encoded small RNA <i>in situ</i> hybridisation, Ventana Benchmark ISH system and an ISH iView kit	Ventana Medical Systems, Tucson, AZ, USA	<a href="https://dmecon.moh.gov.vn/documents/10182/41238806/upload_00002720_1677576294512.pdf?version=1.0&amp;filed=41275971">https://dmecon.moh.gov.vn/documents/10182/41238806/upload_00002720_1677576294512.pdf?version=1.0&amp;filed=41275971</a>
<b>Deposited data</b>		
16S ribosomal RNA sequencing	This paper	Accession number SRA: RJNA820902
Single cell RNA sequencing	This paper	Accession number GEO: GSE229379
<b>Software and algorithms</b>		
Cell Ranger v3.0.1	Zheng et al. <sup>46</sup>	<a href="https://www.10xgenomics.com/">https://www.10xgenomics.com/</a>
Seurat v4.1.1	R Core Team	<a href="https://cran.r-project.org/">https://cran.r-project.org/</a>
Demuxlet	Kang et al. <sup>47</sup>	<a href="https://github.com/statgen/demuxlet">https://github.com/statgen/demuxlet</a>
Sctransform v0.3.3	Hafemeister and Satija <sup>48</sup>	<a href="https://github.com/satijalab/sctransform">https://github.com/satijalab/sctransform</a>
enrichR	Chen et al. <sup>49</sup>	<a href="https://maayanlab.cloud/Enrichr/">https://maayanlab.cloud/Enrichr/</a>
GSEA v4.2.3	Subramanian et al. <sup>50</sup>	<a href="https://www.gsea-msigdb.org/gsea/index.jsp">https://www.gsea-msigdb.org/gsea/index.jsp</a>
immunarch v1.0.0	Robertson et al. <sup>51</sup>	<a href="https://immunarch.com/">https://immunarch.com/</a>
QIIME2 v	Bolyen et al. <sup>52</sup>	<a href="https://qiime2.org/">https://qiime2.org/</a>

**RESOURCE AVAILABILITY**

**Lead contact**

Further information and requests for resources should be directed to and will be fulfilled by the lead contact, Minkyu Jung ([minkjung@yuhs.ac](mailto:minkjung@yuhs.ac)).

### Materials availability

This study did not generate new unique reagents.

### Data and code availability

The microbiota sequencing data and the single cell RNA sequencing data have been deposited to the NCBI sequence read archive database under accession number PRJNA820902 and GSE229379, respectively. All data relevant to the study are included in the article or uploaded as supplementary information. This study did not generate new original code. Any additional information required to reanalyze the data reported in this work paper is available from the Lead Contact upon request.

## EXPERIMENTAL MODEL AND SUBJECT DETAILS

### Patients

This study was based on five independent cohorts (four ICI cohorts and one cytotoxic chemotherapy cohort), namely retrospective exploratory, retrospective validation, prospective validation, experimental stool/blood analysis, and retrospective chemotherapy cohorts (Figure 1). For the retrospective exploratory cohort, we retrieved data from 152 patients with recurrent and/or metastatic AGC who were treated with an anti-PD-1 antibody (pembrolizumab or nivolumab) as a single agent at a tertiary academic center (Yonsei Cancer Center, Seoul, Republic of Korea) between January 2014 and July 2021 (Table 1). For the chemotherapy cohort, we retrieved data from 101 patients with recurrent and/or metastatic AGC who were treated with chemotherapy with a single agent irinotecan at Yonsei Cancer Center between January 2014 and July 2021 (Table 1). For the retrospective validation cohort, we retrieved data from 123 patients with recurrent and/or metastatic AGC who were treated with an anti-PD-1 antibody (pembrolizumab or nivolumab) as a single agent at another tertiary referral center (Gangnam Severance Hospital, Seoul, Republic of Korea) between January 2014 and July 2021 (Table S3). For the prospective validation cohort, we retrieved data from 30 patients with recurrent and/or metastatic AGC who were enrolled in prospective phase II or phase III clinical trials exploiting an anti-PD-1 antibody (pembrolizumab or nivolumab) as a single agent at Yonsei Cancer Center between January 2014 and December 2015 (Table S4). For the experimental stool/blood analysis cohort, we explored data from 24 patients with recurrent and/or metastatic AGC who were enrolled in a prospective cohort study for blood and stool sampling and treated with an anti-PD-1 antibody (pembrolizumab or nivolumab) as a single agent at Yonsei Cancer Center between March 2020 and July 2021 (Table S8). We collected data on the following variables: age at the beginning of treatment, gender, differentiations, human epidermal growth factor-2 (HER-2) expression, microsatellite instability or mismatch repair deficiency status, Epstein-Barr virus association, PD-L1 expression in tumor tissue, previous history of gastrectomy, prior treatments, details of ATB prescription, and treatment outcome including response and survival. Details of ATB prescription were investigated based on the electronic health records system of each center. This study was approved by the institutional review board of Yonsei University College of Medicine (IRB number: 4-2020-0153, 4-2021-0449). Written informed consents were obtained from participants in the prospective validation and experimental stool/blood analysis cohorts. Patient consents were waived for retrospective exploratory, retrospective validation, and retrospective chemotherapy cohorts.

### Follow-up and response evaluation

Laboratory tests and physical examinations were performed at each cycle of treatment administration. Treatment response was evaluated by analysing images, including computed tomography or magnetic resonance imaging scans. Based on the Response Evaluation Criteria in Solid Tumors ver 1.1, treatment response was classified as complete response (CR), partial response (PR), stable disease (SD), or progressive disease (PD).<sup>53</sup> The objective response rate and disease control rate were defined as the proportion of patients with CR and PR, and those with CR, PR, and SD as their best response, respectively.

## METHOD DETAILS

### Evaluation of tumor tissue

Immunohistochemistry (IHC) was performed using a Ventana XT automated staining instrument (Ventana Medical Systems, Tucson, AZ, USA). The following antibodies were used in accordance with the manufacturer's instructions: HER-2 (HercepTest Kit; Dako, Santa Clara, CA, USA), MutL homolog 1 (MLH1; clone M1; Roche, Indianapolis, IN, USA), MutS protein homolog 2 (MSH2; clone G219-1129; Roche, Indianapolis, IN, USA), MutS homolog 6 (MSH6; clone 44; Cell Marque, Rocklin, CA, USA), post-meiotic segregation increased 2 (PMS2; clone MRQ28; Cell Marque, Rocklin, CA, USA), and PD-L1 (clone 22C3; Dako, Santa Clara, CA, USA). PD-L1 expression was quantified using the tumor proportion score (TPS; PD-L1 positivity on tumor cells) or combined positive score (CPS; ratio of overall PD-L1 positivity to PD-L1 positivity on tumor cells), as previously described.<sup>5,54</sup> Amplification of *ERBB2* was explored via silver *in situ* hybridisation (ISH) in case of HER-2 2+ by IHC, as previously described.<sup>55</sup> Epstein-Barr virus-encoded small RNA ISH was performed using a Ventana Benchmark ISH system and an ISH iView kit (Ventana Medical Systems, Tucson, AZ, USA). Microsatellite analysis was performed using DNA extracted from tumor tissues, as previously described.<sup>56</sup> Tumors with microsatellite instability-high/mismatch repair deficient were defined as those with the presence of at least two of the five instability markers in the Bethesda microsatellite panel (BAT25, BAT26, MFD15, D2S123, and D5S346) or the absence of one or more proteins (MLH1, MSH2, MSH6, and PMS2) based on IHC staining.

### 16S ribosomal RNA sequencing with stool samples

Fresh stool samples from the participants were collected using a commercial fecal sampling kit after acquisition of informed consent (OMNIgene GUT; DNA Genotek, Ontario, Canada) and stored at  $-80^{\circ}\text{C}$  prior to DNA extraction for gut microbiota-profiling analysis. The bacterial genomic DNA was extracted from the fecal samples according to the instruction of the QIAamp DNA stool Mini kit (Qiagen, Hilden, Germany). The V3/V4 hypervariable region of 16S rRNA genes was amplified and sequenced using the Illumina MiSeq 2 × 300 System (Illumina, San Diego, CA, USA) according to the manufacturer's instructions. Raw sequencing reads were analyzed by QIIME 2 pipeline.<sup>52</sup> Briefly, raw sequence data were demultiplexed and quality filtered using the DADA2 plugin.<sup>57</sup> The following filtration steps were conducted in addition. Only the features belonging to the bacteria domain and in the range from 380 to 450 base pairs were considered. The filtering step was implemented to remove reads attributed to mitochondria, chloroplasts, and eukaryotes, ensuring that subsequent analyses were limited to the desired microbial sequences. *De novo* chimera filtration was performed using the "vsearch uchime-denovo" program.<sup>58</sup> After the completion of the filtering step, taxonomical assignment was done using a pre-trained Naïve Bayes classifier against the Silva-138 reference sequences. Species assignment was done with "vsearch usearch\_global" based on 99% identity. We obtained an average of 84194.6 16S rRNA sequences from 24 samples after performing quality filtering procedures. Based on the 34,464 smallest reads, we applied rarefaction to standardize the dataset.

### scRNA-seq with circulating immune cells

Peripheral blood mononuclear cells were isolated from venous blood after acquisition of informed consent as described previously.<sup>12</sup> Libraries for scRNA-seq were generated using the Chromium Next GEM Single Cell 5' Kit v2 (10× Genomics, Pleasanton, CA, USA) and Chromium Single Cell Human TCR Amplification Kit (10× Genomics) to read 5'-mRNA and full-length paired T cell and B cell receptor sequences following the manufacturer's instructions. Libraries were constructed and sequenced at a depth of approximately 50,000 reads per cell using the Novaseq 6000 platform (Illumina, San Diego, CA, USA). Data processing and cell type annotation through marker gene identification in each cluster were performed as described previously.<sup>59</sup>

### QUANTIFICATION AND STATISTICAL ANALYSIS

For continuous variables, a Shapiro-Wilk test was performed to determine whether variables were normally distributed or not. An unpaired t-test was used to compare differences between two groups. Additionally, the Wilcoxon rank-sum test was performed for non-normally distributed variables. For categorical variables, the Chi-square test was performed to compare between groups. The Fisher's exact and Mantel-Haenszel Chi-square tests were also performed if indicated. PFS was defined as the time from the initiation of treatment to disease progression or death. OS was defined as the time from the initiation of treatment to death from any cause. The Kaplan-Meier method was used to depict survival distributions, and log rank test was used for comparison. The Cox proportional hazards model was used in univariable and multivariable analyses to assess the significant prognostic factors associated with PFS and OS, with the HR and 95% CIs. Variables with a level of significance for the univariable analyses ( $P$ -values  $<0.05$ ) were included in multivariable analyses. Each Cox regression model for multivariable analyses was tested for proportional hazards assumption using Schoenfeld residuals against transformed time, and the significances of all Cox proportional hazard assumptions were met with  $P$ -values  $>0.05$ . Optimal cut-off values for the therapeutic window of pATB administration before the first administration of nivolumab, pembrolizumab, or irinotecan to predict PFS were derived by log rank maximization method. Based on the cut-off values with log rank maximization method, patients were classified into two groups based on whether they had received pATB during this window (pATB and non-pATB groups). To compare the differences in the gut microbial community among the groups, permutational multivariate analysis of variance (PERMANOVA) implemented in QIIME2 was performed on an unweighted UniFrac distance. Significance of PERMANOVA was obtained by 999 permutation tests. The censoring date was 31 December 2021. Results were considered significant at  $P$ -values  $<0.05$ . All statistical analyses were performed and visualized using GraphPad Prism version 7.0 (GraphPad Software, CA, USA) or IBM SPSS version 25.0 (IBM Corp., NY, USA).